Magazine of Civil Engineering

ISSN 2712-8172

journal homepage: http://engstroy.spbstu.ru/

Research article

UDC 624.139

DOI: 10.34910/MCE.140.9

Determining the temperature of soil under a building with a ventilated basement

M.I. Nizovtsev ✉ , ***A.N. Sterlyagov***

Kutateladze Institute of Thermophysics, Novosibirsk, Russian Federation

✉ *nizovtsev@itp.nsc.ru*

Keywords: permafrost, soil freezing and thawing, soil moisture, radiation balance, building with ventilated basement, calculation model.

Abstract. This work is aimed at computational comparative studies of natural changes in soil temperature and under a building with a ventilated basement in Norilsk. In contrast to conventional projects, it was planned to locate a small part of the building directly on the ground, which could lead to additional thawing of the soil. Laboratory data on soil samples in the thawed and frozen state, taken from boreholes at the construction site, and the results of soil temperature measurements at a depth of about 14 m were used to perform calculations. When forming the boundary conditions of the calculation model on the outer surface of the soil, the radiation balance for the conditions of Norilsk was considered. It was found that the radiation balance from May to August is positive and leads to soil heating, and in the rest, most part of the year, it is negative and causes soil cooling. New results obtained demonstrate that a decrease in the moisture content of the surface soil layers reduces the influence of phase transitions on the thermal-inertial properties of the soil, which leads to an increase in the thickness of the active soil layer (where annual temperature fluctuations are observed), an increase in the depth of thawing in the summer-autumn period, and a decrease in the soil temperature under the active layer. The temperature distributions over the depth of soil under different sections of the building with a ventilated basement and in the immediate vicinity of the building in a long-term operation cycle after completion of its construction were calculated. According to calculation results, the maximum depth of soil thaw under a building with a ventilated basement decreased by 12 % compared to natural conditions, reaching 1.1 m. It is shown that for multi-story buildings with ventilated basements, individual structural elements with insulation can be located directly on the ground surface, and additional thawing of the soil will not occur under them. However, for this case, the absence of additional thawing of soil should be confirmed by a heat engineering calculation taking into account the ratio of surface areas of the ventilated basement and the structural elements located on the ground, as well as the features of their insulation.

Funding: The work was carried out within the framework of the state assignment of the IT SB RAS (project No. 126021217057-2).

Citation: Nizovtsev, M.I., Sterlyagov, A.N. Determining the temperature of soil under a building with a ventilated basement. Magazine of Civil Engineering. 2025. 18(8). Article no. 14009. DOI: 10.34910/MCE.140.9

1. Introduction

The object of study of this work is the distribution of temperature in permafrost soils in the annual cycle during the construction of buildings with a ventilated basement in Norilsk.

According to expert findings, the actual area of permafrost is 15 % of the land area in the Northern Hemisphere and 0.5–0.6 % in the Southern Hemisphere [1]. In Russia, about 60–65 % of the land surface,

which is 11 mln km^2, is presented by permafrost zones, and permafrost is continuously distributed over 85 % of the Arctic zone [2].

The Russian Arctic is one of the most urbanized regions of Russia with the urban population accounting for about 88 % [3]. There are six cities in the Russian Arctic with a population of over 100,000 people: Murmansk, Arkhangelsk, Severodvinsk, Novy Urengoy, Noyabrsk, and Norilsk. In these cities, a large number of multi-story buildings have been built and are in operation. Cities in the Arctic are heat islands in regions with a cold continental climate, where the average annual surface temperature of the earth is approximately 6 °C higher than the surface temperature of the soil under natural conditions.

The general trend of climate warming is also manifested by an increase in permafrost temperature in different regions of the world [4]. The temperature regime of permafrost is usually characterized by the average value of annual temperature measured at a depth of zero annual soil temperature amplitudes, which is usually 10–15 m in the northern regions of Western Siberia. The observed warming for permafrost soil in the Arctic region is 2.8 °C, which corresponds to the average annual temperature increase of 0.056 °C/year. In the European north of Russia, the increase in permafrost temperature is slower and is 0.04 °C/year [5]. Thus, Arctic permafrost is warming faster, which is associated with a more significant increase in the air temperature in the Arctic region [6].

Some studies have modeled the average annual change in shallow permafrost temperature associated with warming. Thus, modeling performed for the western part of the Yamal Peninsula showed that the average annual change in soil temperature could reach a depth of 50 m in the next 50 years, while permafrost could become 1.3 °C and 2.3 °C warmer at depths of 20 m and 7–10 m, respectively [7]. The current trend of climate warming will obviously continue, which is confirmed by modeling of the general circulation in the atmosphere [8].

If the warming trend does not change to cooling by the end of the 21st century, most of the underground permafrost will melt, leading to irreversible changes in the landscape and destruction of the built environment [9]. The damage from permafrost thawing in Russia by 2050 is estimated to be around 105 billion dollars [10].

Almost 4,000,000 people, about 70 % of the existing infrastructure, and 45 % of hydrocarbons in the Russian Arctic are located in areas with a high potential for melting of near-surface permafrost and associated risks of soil instability by 2050 [11].

Design and construction of structures in permafrost regions requires consideration of global warming trends and the associated increase in permafrost temperature. Permafrost warming can change its properties due to an increase in the content of unfrozen pore water, which can be unevenly distributed in heterogeneous permafrost. Unfrozen water can exist in soils over a wide range of negative temperatures. The liquid component of pore moisture has been the subject of research for about 100 years, but many aspects of the problem remain poorly understood, including control of the phase composition of moisture in permafrost [12] and the influence of surface soil moisture on the depth of soil thawing during the summer-autumn period.

Although the temperature of permafrost in the Northern Hemisphere reaches –12 ÷ –10 °C, some part of the pore moisture remains unfrozen [13].

Prolonged warming in the Arctic is accompanied by a gradual increase in the temperature of the near-surface permafrost and an associated increase in the content of unfrozen water at the depths reached by heat waves. These processes cannot be classified as melting, since the soil does not become completely thawed and remains at negative temperatures, although it contains a large amount of unfrozen water. Thus, permafrost degradation actually occurs [12].

The amount of unfrozen pore water depends on the soil salinity and peat content; it is much greater in saline and peat-rich soils than in non-saline rocks with a lack of organic matter [14]. These soil features must be taken into account when operating existing engineering structures and when preparing new projects.

Permafrost retains a huge cold resource and is unlikely to melt to a catastrophic degree in the coming decades. However, constant warming of the near-surface permafrost can change the phase composition of the pore moisture due to an increase in unfrozen water, and this will cause transition of the solid permafrost into a more plastic state. The content of unfrozen water can increase even more as a result of thermal impact during the construction of buildings and structures, drilling operations, laying pipelines, etc. [15].

The widespread occurrence of permafrost in the Arctic region and the extremely harsh climate create great difficulties during construction [16]. There are a number of proven technologies for constructing facilities in Arctic conditions, and the technology of using a ventilated basement in buildings is one of the most common among them. This technology ensures heat removal from the building and prevents its

penetration into the soil [17]. Measurements of soil temperature distribution under a building with a ventilated basement in the city of Yakutsk showed that soil cooling was especially significant in the first two to three years after the completion of construction: by 3–4 °C and 0.3 °C at the depths of 6 m and 18 m, respectively. During the construction of buildings with ventilated basements, a decrease in soil temperature under them was 3–6 °C in Norilsk, 1–3 °C in Yakutsk [18], and 0.5–1.5 °C in Igarka [19]. In addition, the technologies of injection soil stabilization and improvement of soil properties by jet grouting are also used [20]. Therefore, there are limited data in the literature on the reduction of soil temperature under buildings with ventilated basement, but there are no results of such measurements over a long period of time with a detailed description of the composition and properties of the soils.

One of the methods for creating industrial infrastructure on permafrost soils is the method of pile foundation, which is erected in winter with preliminary soil strengthening [21]. The developers of this method calculate possible warming scenarios that may result in a decrease in the bearing capacity of piles, using the software package “Frost 3D”. In the case of a risk of a significant reduction in the bearing capacity, it is suggested to use thermosiphons for additional soil freezing.

Construction of infrastructure in permafrost regions can cause changes in the properties of permafrost. Laying highways and constructing embankments over permafrost inevitably lead to the changes in local microclimate conditions and affect the surrounding vegetation, snow cover, and soil water balance [22].

To analyze the state of permafrost, it is proposed to use a method based on the application of freezing and thawing indices applying the results of the field measurements in soils at construction sites [23]. Such an analysis of the numerical values of the indices allows an estimate of the final impact of the entire spectrum of anthropogenic and natural factors on the state of permafrost. The development of numerical methods for predicting the strength of permafrost [24] and the processes of formation of frost cracks, taking into account changes in temperature fields and the physical and mechanical properties of permafrost is an important issue [25].

The results of comparative calculations of the depth of soil freezing performed with application of engineering calculation methods, as well as numerical methods, using the software packages “Frost 3D” and “Borey 3D”, widely applied in Russia for permafrost soils, are presented in [26]. Based on this work, it was concluded that for further improvement of calculation methods, an increase in their accuracy and further development, it is necessary to use them together with the field measurements.

In particular, this research was aimed at computational studies of changes in soil temperature under a building with a ventilated basement, whose construction is planned on permafrost soils in Norilsk. In contrast to conventional projects, this project plans to locate a small part of the building directly on the ground. Data of laboratory studies of soil samples in the thawed and frozen state, taken from boreholes at the construction site, as well as the results of measuring soil temperatures at a depth of about 14 m, were used in calculations. Another objective set in this work was to consider the effect of soil moisture and associated phase transitions of pore moisture during freezing and thawing of the soil on the temperature distribution in permafrost soils in a long-term observation cycle.

When constructing various industrial and residential facilities on permafrost soils, the problems associated with specific design solutions arise. So, this calculation study was started by the project for the construction of a multi-story residential building in Norilsk. The multi-story residential building, like many facilities in Norilsk, is supposed to be built with a ventilated basement to prevent thawing of the permafrost soil underneath it (Fig. 1), but the small elevator area compared to the total area of the building (Fig. 2) is located on reinforced concrete blocks installed directly on the ground. The floor of the elevator is insulated with a 200 mm thick layer of extruded polystyrene foam. Thus, the question about possible thawing of soil under the elevator arose.

Figure 1. Ventilated underground space of a residential building on permafrost soil.

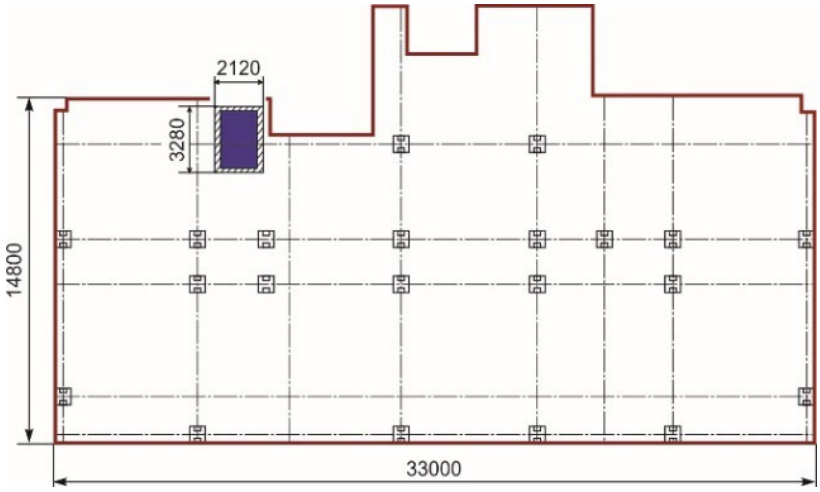

Figure 2. Floor framing plan of the 1st floor.

It was decided to expand the question posed and consider the following set of tasks when performing computational studies:

- to determine the natural temperature changes in the annual cycle over the soil depth and a temperature change under a ventilated basement in the conditions of Norilsk;
- to determine the greatest depth of soil thawing under these conditions;
- to find out the effect of phase transformations of moisture in the soil during cyclic processes of freezing and thawing on the temperature distribution in permafrost soil;
- to determine the dynamics of changes in the distribution of soil temperature in different zones under a residential building with a ventilated underground and under an elevator located on reinforced concrete blocks installed directly on the ground.

2. Methods

The calculations were carried out using the software packages “Frost 3D” and “Borey 3D”, designed to perform non-stationary numerical thermal calculations in multilayer soils taking into account the processes of their freezing and thawing. The processes of heat distribution in the soil with phase transformations can be described by a differential equation written in the enthalpy form [27]:

$$\frac{\partial H}{\partial \tau} = div\left(\lambda \times gradT\right) + f, \tag{1}$$

where $H\left(\tau, T\right)$ is the enthalpy of unit volume of soil, τ is time, T is the soil temperature, $\lambda\left(T\right)$ is the coefficient of soil thermal conductivity, and $f\left(\tau\right)$ is the power of internal heat sources.

Taking into account the phase transitions in the soil:

$$H\left(T_1\right)=\int_0^{T_1}\left[C\left(T\right)+Q\times\delta\left(T-T_{of}\right)dT\right], \tag{2}$$

where $C\left(T\right)$ is the volumetric heat capacity of soil, Q is the heat of phase transition, T_{of} is the temperature at onset of freezing, $\delta\left(T-T_{of}\right)$ is the delta-function.

$$C_{eff}=C_f+\rho_{df}L\frac{\partial W_w}{\partial T}, \tag{3}$$

where C_f is the heat capacity of soil in frozen state, W_w is humidity due to unfrozen water, ρ_{df} is the density of dry soil, and L is the specific heat of ice melting.

The coefficient of soil thermal conductivity depends on temperature in the following manner:

$$\lambda\left(T\right)=\begin{matrix}\lambda_{th},\ T>T_{of}\\ \lambda_{eff},\ T<T_{of}\end{matrix}, \tag{4}$$

where λ_{th} is the coefficient of thermal conductivity of thawed soil and λ_{eff} is the coefficient of effective thermal conductivity of frozen soil.

$$\lambda_{eff}=\lambda_f-\frac{\lambda_f-\lambda_{th}}{W_{tot}-W_{w\lambda}}\left(W_w-W_{w\lambda}\right), \tag{5}$$

where λ_f is the coefficient of thermal conductivity of frozen soil, W_{tot} is the total soil humidity, and $W_{w\lambda}$ is the humidity due to unfrozen water at determination temperature λ_f.

A change in the moisture content during soil freezing was taken into account in calculations depending on the soil type and its temperature, according to [28]. A decrease in the content of unfrozen moisture in the soil during its freezing depends on the type of soil. According to the degree of an increase in the proportion of unfrozen moisture in soils during freezing, the following sequence is observed: filled soil, sandy clay, clay loam, and clay (Fig. 3a). Peat should be singled out separately: usually it has higher moisture content and larger amount of unfrozen moisture at negative temperatures (Fig. 3b).

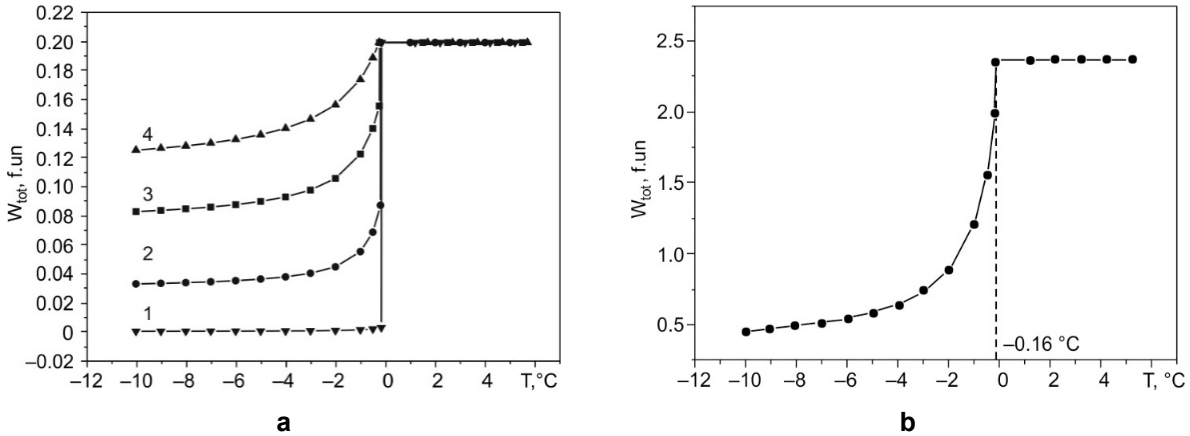

Figure 3. A change in total soil moisture during freezing:
a) 1 – filled soil, 2 – sandy clay, 3 – clay loam, 4 – clay; b) peat.

The dependence of the amount of unfrozen water on soil temperature depends on the soil type and its temperature at onset of freezing T_{of}. For soil temperatures $T>T_{of}$, a constant value of the amount of unfrozen water W_{tot} was adopted. This value, like the freezing onset temperature T_{of}, was determined based on laboratory measurements for each soil type. For soil temperatures $T\le T_{of}$, the dependence of the amount of unfrozen water on temperature was determined in the software package as a calculation curve based on SP 25.13330.2025 and approximated as a function:

$$W_w(T) = A + B/(C - T), \tag{6}$$

where A, B and C are the approximation parameters, T is the soil temperature, °C.

Thus, over the entire temperature range, the dependence of the amount of unfrozen water on the soil temperature was described by the expression:

$$W_w(T) = \begin{matrix} W_{tot}, & T \geq T_{of} \\ A + B/(C - T), & T \leq T_{of} \end{matrix}. \tag{7}$$

Solar radiation is one of the main factors influencing the soil temperature. Let us consider the radiation balance of the soil surface R:

$$R = (W_{dir} + W_{dif})(1 - A) - l_{eff}, \tag{8}$$

where W_{dir} and W_{dif} are the powers of direct and diffuse solar radiation reaching the soil surface, A is the surface albedo, and l_{eff} is the effective power of long-wave surface radiation [29]:

$$l_{eff} = l_{eff.0}\left(1 - c \times n^2\right) + 4\varepsilon\sigma T^3 (T_{sur} - T); \tag{9}$$

$$l_{eff.0} = \varepsilon\sigma T^4 \left(0.39 - 0.058\sqrt{(e/133.32) \times 6.973 \cdot 10^{-6}}\right) \text{ is the dependence of M.E. Berlyand,} \tag{10}$$

where $l_{eff.0}$ is the effective power of long-wave radiation of the surface without taking into account clouds, W/m²; ε is the surface emissivity coefficient; σ is the Stefan-Boltzmann constant; e is the partial pressure of water vapor, Pa; n is the cloud cover; and c = 0.80 at 69 latitude.

Let us determine the radiation balance of the Earth surface during the year in Norilsk using long-term observation data [30]. The data on distribution of the average power of total solar radiation falling on the surface (1), the surface albedo (2), and the average power of solar radiation absorbed by the surface taking into account its reflective properties (3) are shown in Fig. 4. According to the observations, the average monthly power of solar radiation in the summer in the conditions of Norilsk did not exceed 220 W/m², and the power absorbed by the soil taking into account the surface albedo was less than 180 W/m².

The annual distribution of the effective long-wave radiation power of the surface under clear skies $I_{eff.0}$ taking into account the cloud cover according to data of [31] is shown in Fig. 5. In summer, the effect of the cloud cover has a smaller screening effect on long-wave cooling of the surface than in other periods of the year, and the effective long-wave radiation power of the surface exceeds 60 W/m².

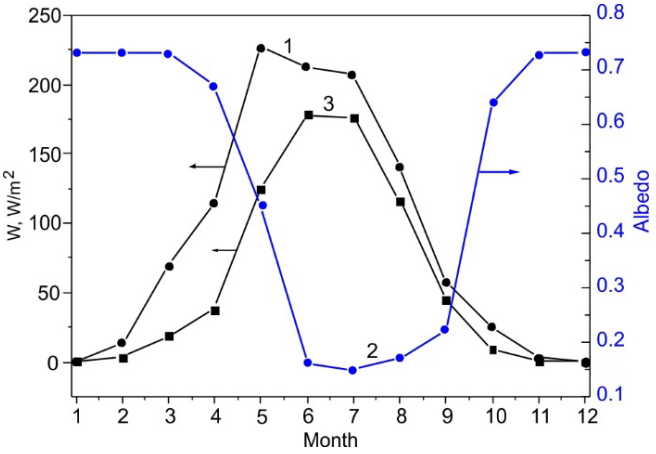

Figure 4. Average power of total solar radiation: 1 – falling on the surface, 3 – absorbed by the surface. 2 – albedo of the surface.

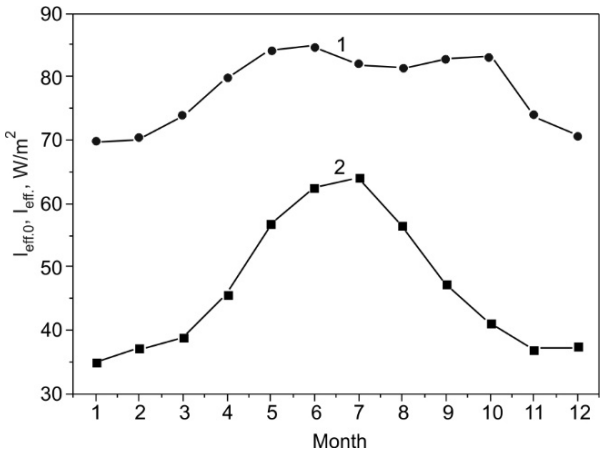

Figure 5. Average power of effective long-wave radiation of the surface: 1 – $I_{eff.0}$, 2 – I_{eff}.

Let us determine the heat flux on the outer surface:

$$Q_{sur} = R + Q_{con} - Q_{eva}, \tag{11}$$

where Q_{con} is the convective heat flux over the surface, Q_{eva} is the heat flux from the soil surface associated with moisture evaporation, which can be approximately determined, $Q_{eva} = mL$, where m is the mass of precipitation per 1 m^2 in the form of rain, and L = 2.5×10^6 J/kg is the heat of water evaporation.

The distribution of the average radiation balance during the year, as well as the radiation balance together with heat removal from the soil surface during moisture evaporation are shown in Fig. 6. According to the results presented, from May to August, the radiation balance is positive and leads to soil heating, and during the rest of the year, it is negative and causes soil cooling.

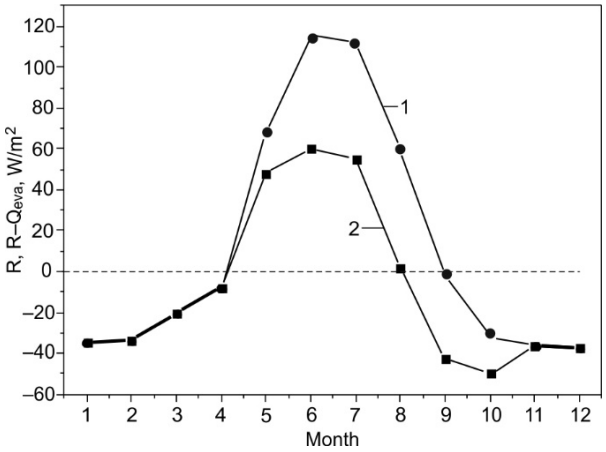

Figure 6. Average values over the year: 1 – *R*, 2 – *R* – Q_{eva}.

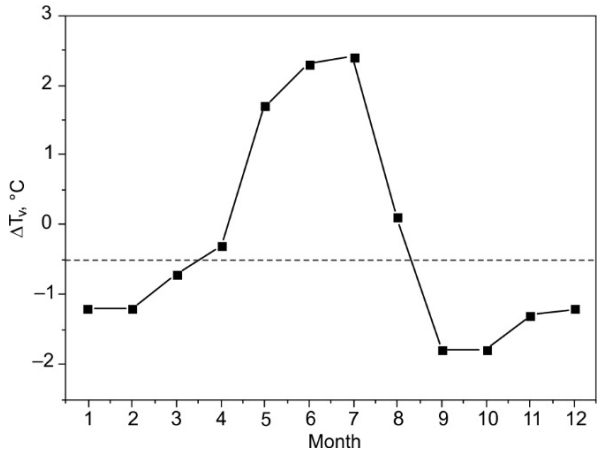

Figure 7. Calculated correction to the average monthly air temperature.

During calculations, the following heat flux was specified on the outer surface of the soil:

$$Q_{s.sur} = k\left(T^* - T_{s.sur}\right), \tag{12}$$

where k is the heat transfer coefficient taking into account a snow layer on the soil surface.

$$k = 1/\left(1/\alpha_{con} + d_s/\lambda_s\right), \tag{13}$$

where α_{con} is the convective heat transfer coefficient taking into account the wind speed, d_s is the snow layer thickness [32], and λ_s is the thermal conductivity coefficient of snow, T^* is the effective air temperature taking into account the radiation balance and moisture evaporation from the soil surface:

$$T^* = T_v + \Delta T_v = T_v + \left(R - Q_{eva}\right)/\alpha_{con}. \tag{14}$$

The resulting calculated correction to the average monthly air temperature ΔT_v for the climatic conditions of Norilsk is shown in Fig. 7. In the summer months, when calculating soils, this correction increases the average monthly air temperature by up to 3 °C, and in the winter months, on the contrary, it decreases it by 1–2 °C.

In calculations, a soil body with a thickness of 50 m was considered, and adiabatic conditions $\left(Q = 0\right)$ were assumed on its lower surface, which is well confirmed by the results of the field measurements.

To calculate the temperature change over the soil depth under different boundary conditions, the data on the soil composition and the thickness of soil layers were taken from the technical report on the results of engineering and geological surveys at the construction site of a multi-story residential building in Norilsk. A total of 10 boreholes were drilled at the construction site and soil samples were taken. The data from one of the boreholes with a description of soils, the depth and thickness of layers, and the distribution of soil temperature over the depth at the beginning of June 2023 are presented as an example in Fig. 8.

Absolute mark 48.7 m
Depth 14.20 m
Drilling date 19.04.2023

EGE No.	Abs. mark	Depth of occurrence	Thickness	Soil description
1	47.60	1.10	1.10	Filled soil
2	46.70	2.00	0.90	Peat, moderately decomposed
3	43.80	4.90	2.90	Clay loam of layered cryogenic structure, frozen, non-saline
4	38.60	10.10	5.20	Clay of layered cryogenic structure, frozen, non-saline, with inclusion of crushed stone
5	38.20	10.50	0.40	Clay loam of layered cryogenic structure, frozen, with inclusion of crushed stone, non-saline
6	36.50	12.20	1.70	Soil with crushed stones of layered cryogenic structure, frozen, non-saline with sandy loam filler
7	34.50	14.20	2.00	Dolerite (basalt), slightly cracked, slightly weathered, medium strength

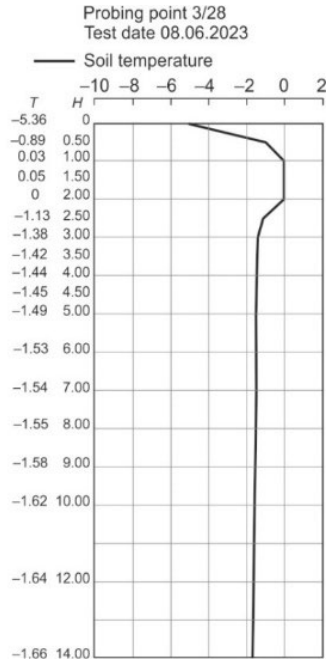

Figure 8. Data for one of the boreholes.

Based on the survey results, seven types of soils were identified. The soil temperature at a depth of 14 m remained almost unchanged and was approximately –1.7 °C. The list of all soil types according to their location from the surface with indication of their thickness based on the results of averaging information from 10 boreholes is presented in Table 1.

Table 1. Types and average thickness of soil layers.

Soil No.	Description of soils	Layer thickness, m
1	Filled soil	1.49
2	Peat, moderately decomposed	0.84
3	Clay loam of layered cryogenic structure, frozen, non-saline	2.9
4	Clay of layered cryogenic structure, frozen, non-saline, with inclusion of crushed stone	5.88
5	Clay loam of layered cryogenic structure, frozen, with inclusion of crushed stone, non-saline	0.91
6	Soil with crushed stones of layered cryogenic structure, frozen, non-saline with sandy loam filler	1.3
7	Dolerite (basalt), slightly cracked, slightly weathered, medium strength	below 13.32 m

Based on the results obtained in the specialized soil testing laboratory, the soil properties in the thawed and frozen state are summarized in Table 2, where $\rho_{d.s.}$ is the density of dry soil, λ_f and λ_{th} are the thermal conductivity coefficient of frozen and thawed soil, c_f and c_{th} are the volumetric heat capacity of frozen and thawed soil, W is the soil moisture content, T_{of} is the temperature at onset of freezing.

Table 2. Soil properties.

Soil No.	$\rho_{d.s}$, kg/m^3	λ_f, W/m^{2}K	λ_{th}, W/m^{2}K	c_f, ×10^{-6} J/kgK	c_{th}, ×10^{-6} J/kgK	W, %	$T_{of,}$ °C
1	1800	1.88	1.76	2.32	3	17	0
2	290	1.07	0.62	2.15	3.44	243	–0.2
3	1450	1.63	1.47	2.23	3.07	21.6	–0.2
4	1250	1.8	1.57	2.12	3.10	38.4	–0.25
5	1550	1.66	1.50	2.29	3.12	26	–0.2
6	1810	1.90	1.79	2.34	3.02	17.2	0

The data on the types of soil layers, their average thickness and properties in the thawed and frozen state are used in further calculations to determine the temperature distribution over the depth of the soil under different boundary conditions on its surface.

3. Results and Discussion

At the initial stage, a change in the soil temperature under natural conditions in the annual cycle was calculated for the city of Norilsk. The boundary conditions on the outer surface of the soil were determined taking into account all the factors specified earlier for the climatic conditions of the city of Norilsk, given in Table 3.

Table 3. Climatic Parameters.

Month of the year	Air temperature, °C	Wind speed, m/s	Thickness of snow, ×10^3, m	Rainfall, ×10^3, m	Average total solar radiation power, W/m^2	Surface albedo	Cloudiness
1	–27.6	6	278	0	0.7	0.73	0.78
2	–27.1	5.4	350	0	12.8	0.73	0.76
3	–22.1	6	406	0	69.1	0.73	0.77
4	–13.8	6.1	455	0	115	0.67	0.73
5	–5.3	5.8	365	21.6	227	0.45	0.64
6	6	5	0	57.8	212.2	0.16	0.58
7	14	4.2	0	61.3	207	0.15	0.54
8	10.4	4.1	0	60.4	140.4	0.17	0.63
9	3.6	4.5	0	43	57.5	0.22	0.73
10	–8.7	5.7	101	18.6	24.7	0.64	0.79
11	–22.2	5.5	244	0	3	0.73	0.79
12	–25.7	6.1	286	0	0	0.73	0.77

Calculations were carried out for a soil body 50 m thick. The types of soil layers and their thickness corresponded to Table 1, and the properties of soils in the thawed and frozen state corresponded to Table 2. The initial temperature distribution in the soil was assumed to be constant at –2 °C. The calculation began in mid-October and was performed for a period of 10 years; then, the temperature distribution across the soil thickness was compared with the initial value, and the next iteration of calculation was performed. The calculation was completed, and the regime of the soil temperature change was considered steady-state at a maximum difference in temperature between the initial and final values of < 0.01 °C. On average, the calculation with reaching the steady-state regime covered a time period of about 250 years. The flowchart of the calculation program is shown in Fig. 9.

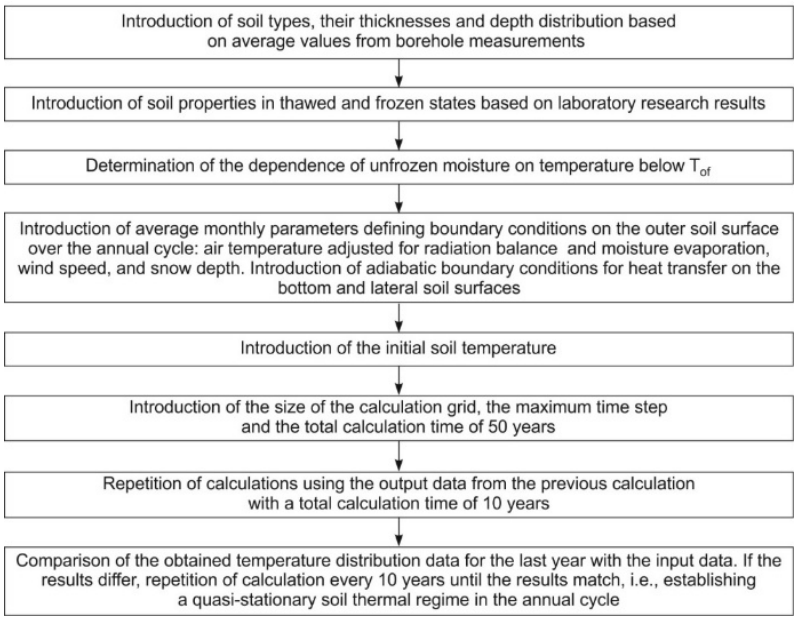

Figure 9. The flowchart of the calculation program.

When reaching a steady-state regime of soil temperature change during the year, soil temperature profiles were determined for the middle of each month. The temperature distributions over the soil depth in February and July, obtained by calculations with average data of long-term measurements for these months in Norilsk, are compared in Fig. 10 [32]. To validate the calculation model quantitatively, the root mean square error (RMSE) between the calculated and average experimental temperatures in Fig. 10 was determined according to the relationship:

$$RMSE = \sqrt{\frac{1}{n}\sum_{i=1}^{n}\left(\frac{T_{calc} - T_{\exp}}{T_{\exp}}\right)^2}, \quad (15)$$

where $T_{\exp}$ is the measured temperature, T_{calc} is the calculated temperature, n is the number of experimental points.

The RMSE between the calculated temperatures and the long-term average experimental temperatures was 0.67 °C for February (Fig. 10a) and 1.68 °C for July (Fig. 10b).

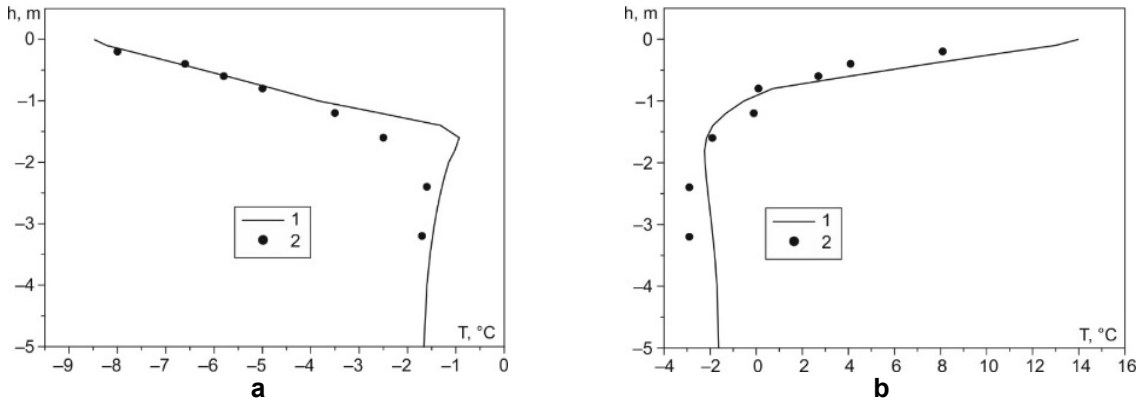

Figure 10. Comparison of temperature distribution under natural conditions: a) February, b) July; 1 – calculation, 2 – measurement data [32].

The results of calculations of changes in distribution of soil temperature over the depth in different months of the year are shown in Fig. 11a.

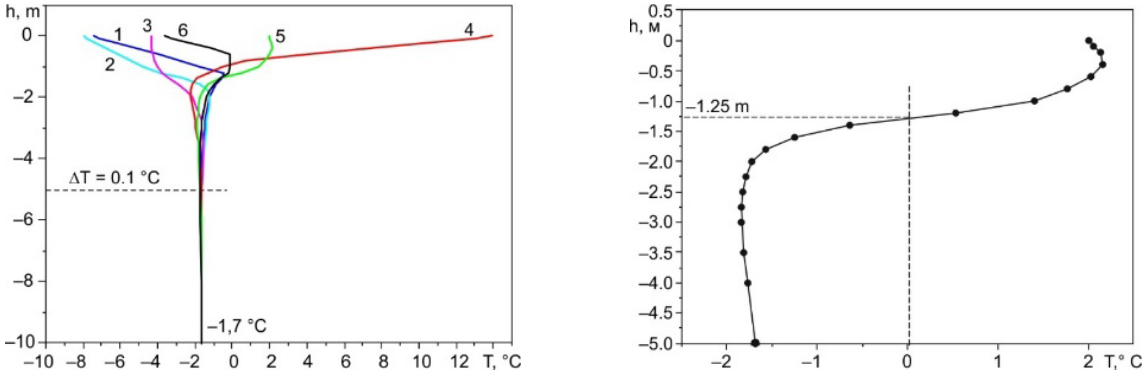

a b

Figure 11. Distribution of soil temperature under natural conditions: a) by month: 1 – January, 2 – March, 3 – May, 4 – July, 5 – September, 6 – November; b) September in detail.

It is possible to distinguish the active soil layer, where the temperature changed during the year. If we conditionally take the soil layer, where the temperature change during the year is ΔT > 0.1 °C, as the active layer; then, according to calculations performed, the boundary of the active layer under natural conditions was at a depth of about 5 m. Below this depth, the soil temperature did not change during the year and it was –1.7 °C, which is in good agreement with the results of actual measurements in boreholes at the construction site of a multi-story residential building (see Fig. 8).

The greatest depth of soil thawing (depth with soil temperature above 0 °C) under natural conditions, according to calculations, was observed in September, and it amounted to 1.25 m (Fig. 11b).

The calculation complexes applied take into account the thermal effects associated with freezing and thawing of moisture contained in the soil, so it is of particular interest to clarify the influence of phase transitions on the temperature distribution in permafrost soils. For this purpose, temperature changes over the soil depth under natural conditions were calculated without taking into account phase transitions during freezing and thawing of moisture, which in practice corresponds to dry soils.

The results of calculations without taking into account phase transitions are presented in Fig. 12.

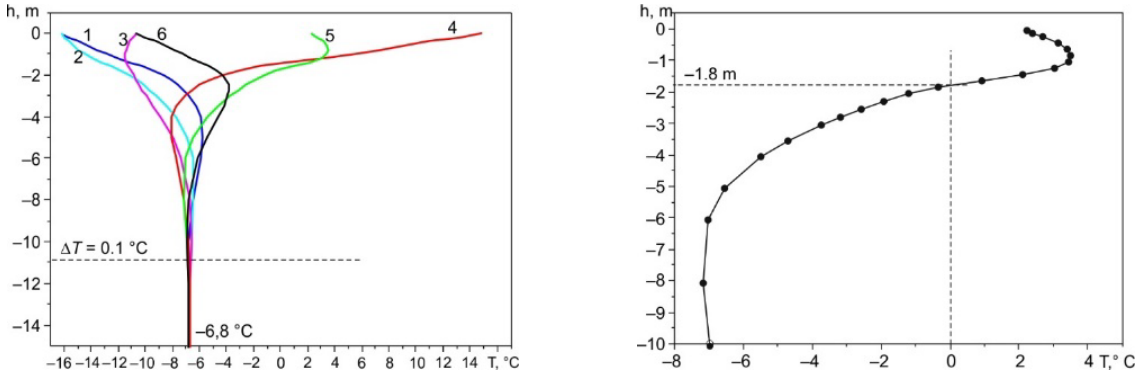

a b

Figure 12. Distribution of temperature in the soil under natural conditions without phase transitions: a) by months: 1 – January, 2 – March, 3 – May, 4 – July, 5 – September, 6 – November; b) September in detail.

Under these calculation conditions, the depth of the active layer increased compared to Fig. 11a by more than twice up to 11 m, and the constant soil temperature at this depth of –6.8 °C decreased significantly. The greatest depth of soil thawing, as in the previous calculation, was observed in September, but it increased by 0.5 m and amounted to –1.8 m (Fig. 12b).

Thus, the calculations showed that the moisture contained in the soil due to phase transitions during freezing and thawing of the soil has a screening effect, reducing the thickness of the active layer with soil temperature changes and the depth of soil thawing in the summer-autumn period, and prevents a general decrease in temperature in the deep soil layers.

When constructing buildings on permafrost soils, the construction technology with the use of a ventilated basement seems to be very good in order to prevent soil thawing and maintain its bearing

capacity (Fig. 1). The change in distribution of soil temperature, when the upper boundary of soil is under the conditions of a ventilated basement of unlimited size, was calculated taking into account the climatic features of Norilsk. The initial temperature distribution in the soil was assumed to be constant at –2 °C.

Unlike the previously considered case, when the soil was under natural conditions, the boundary condition on the outer surface of the soil was changed during the calculations: the absence of snow cover during the cold period of the year and changes in the radiation balance due to the shielding of direct solar radiation and effective long-wave radiation of the soil surface by the building were taken into account.

The results of calculating the change in the distribution of soil temperature in the annual cycle under the conditions of a ventilated basement are presented in Fig. 13.

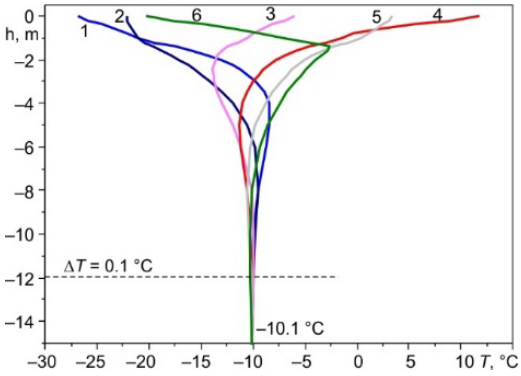

Fig. 13. Temperature distribution in the soil during the year under conditions of a ventilated basement: 1 – January, 2 – February, 3 – March, 4 – April, 5 – May, 6 – June, 7 – July, 8 – August, 9 – September, 10 – October, 11 – November, 12 – December.

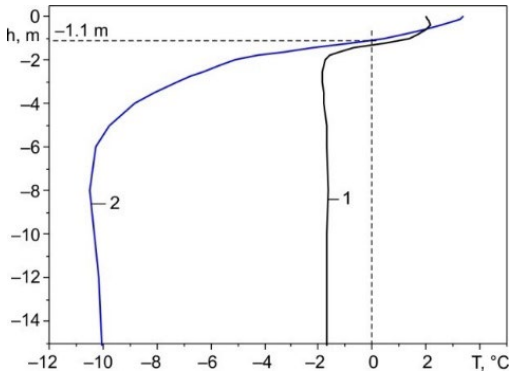

Figure 14. Comparison of the results of temperature distribution calculations in the soil in September: 1 – under natural conditions, 2 – under conditions of a ventilated basement.

When analyzing the results, attention should be paid to two features of a change in the soil temperature distribution during the annual cycle. The first feature is a significant decrease in the soil temperature below the active layer to –10.1 °C compared to the temperature of –1.7 °C, obtained earlier for the soil under natural conditions (see Fig. 11a). The second feature is associated with an increase in the thickness of the active layer of the soil to 12 m compared to the thickness of the active layer of 5 m for the soil under natural conditions. However, despite an increase in the active layer thickness under conditions of a ventilated basement, taking into account the general cooling of the soil, the maximum depth of soil thawing in September even decreased compared to the depth of soil thawing under natural conditions and amounted to –1.1 m (Fig. 14).

Thus, the absence of snow cover and direct solar radiation were the main factors that led to a decrease in the soil temperature under conditions of the ventilated basement of the building compared to the soil temperature under natural conditions and a decrease in the maximum depth of soil thawing in September. Therefore, when choosing the design of a ventilated basement, it is necessary to ensure that the soil surface in the ventilated basement is protected from solar radiation in the summer and is not covered with snow in the winter. Ventilated basement technology for the construction of multi-story buildings on permafrost soils has proven itself in practice and is becoming especially relevant in view of the observed global warming in northern regions.

Let us consider the soil temperature under a residential building with a ventilated basement and an elevator located on reinforced concrete blocks installed directly on the ground. The plan of the 1st floor with the overall dimensions of the ventilated basement and the elevator is shown in Fig. 2. To calculate the soil temperature, a 50 m thick design section was selected. In the central area of its surface, there is a zone

with boundary conditions characteristic of a ventilated basement and a small section of the elevator (Fig. 15).

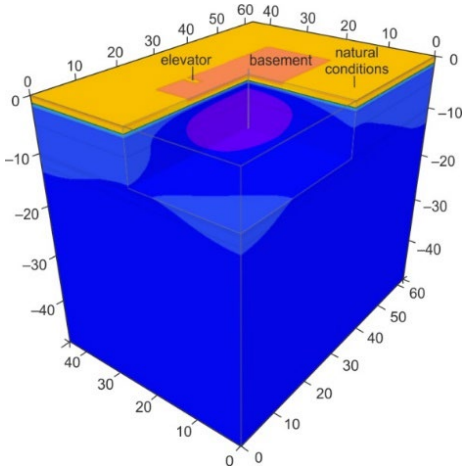

Figure 15. Design section.

In the calculations, it was assumed that the air temperature in the elevator during the heating season was 5 °C, and without heating, the air temperature there was equal to the air temperature outside. The surface area around the building in the figure, highlighted in yellow, corresponded to the soil surface under natural conditions; the length of this section from each side of the building was 15 m. Thus, on the outer surface of the soil, 3 sections with different boundary conditions were identified, while the distribution of soil temperature over the depth was determined at the center of each of these sections. The distribution of the initial soil temperature over the depth in calculations was taken as the temperature distribution obtained under natural conditions.

The distribution of soil temperature in September under a ventilated basement, under an elevator and in a section of soil directly next to the building under natural conditions after 1 year, 5 years, 30 years, and 250 years (the time required to reach a steady state in the annual cycle) from the start of the calculation is presented in Fig. 16.

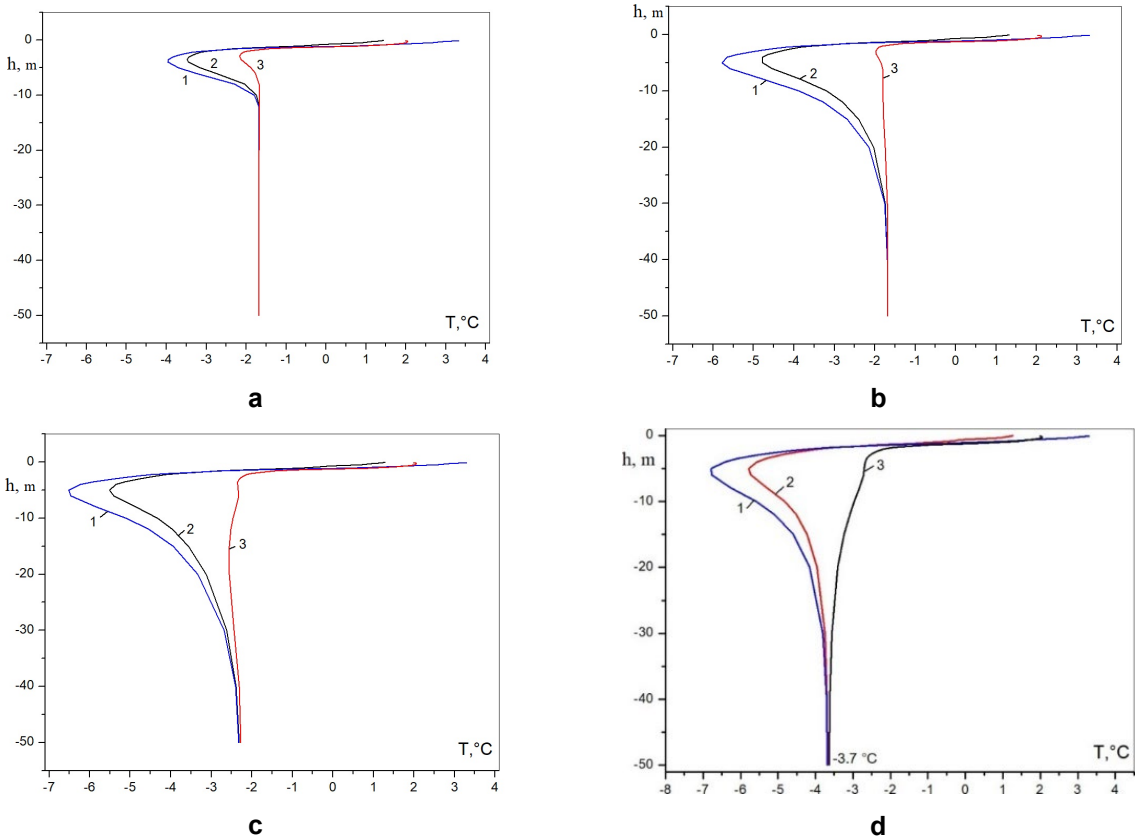

Figure 16. Temperature change in the soil depth after: a) 1 year, b) 5 years, c) 30 years, d) 250 years; 1 – under a ventilated basement, 2 – under an elevator, 3 – near a building.

According to the calculations, after 5 years, the lowest soil temperature was obtained under the ventilated basement, slightly higher temperature was obtained under the elevator, and the highest temperature was obtained near the building. The soil temperatures under all the considered areas converged gradually with increasing soil depth and reached a constant value. The soil temperature at a depth of 50 m after 5 years did not change and was equal to –1.7 °C, which corresponded to the temperature below the active layer for soil under natural conditions (Fig. 16a). After 30 years, a noticeable decrease in temperature was observed throughout the entire depth of the calculated area (Fig. 16c), and after 250 years, the temperature stabilized at a depth of 50 m with a soil temperature of –3.7 °C (Fig. 16d).

To determine the maximum depth of soil thawing, let us consider the temperature distribution in the surface layers of the soil in September with an established annual cycle of soil temperature change (Fig. 17).

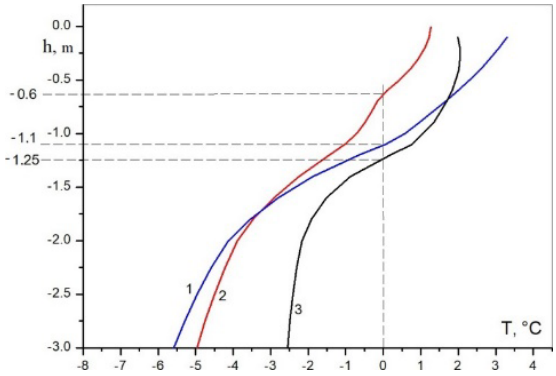

Fig. 17. Determination of the maximum depth of soil thawing: 1 – under a ventilated basement, 2 – under an elevator, 3 – near a building.

The calculation results show that the depth of soil thawing near the building was –1.25 m, under the ventilated basement, it was –1.1 m, and the smallest depth of soil thawing was obtained under the elevator: it was –0.6 m, which is associated, on the one hand, with good insulation of the elevator floor, and, on the other hand, with inertial thermal processes occurring in the soil.

Thus, the calculations performed showed that in multi-story buildings with ventilated basements, constructed in regions with permafrost soils, individual structural elements can be located directly on the ground surface. This will not cause additional soil thawing underneath them; however, in each specific case this should be confirmed by special calculations. When calculating, it is necessary to consider the thermal conditions in the rooms above the structural elements located on the ground, the ratio of the areas of the ventilated basement to the foundation of the structure, and additional insulation from the ground surface. It should be noted that the optimal location for such structures is the central zone of the ventilated basement.

4. Conclusions

The performed calculations of changes in soil temperature during the annual cycle in the climatic conditions of Norilsk using data on the types and thicknesses of soil layers obtained from boreholes, as well as on the basis of the characteristics of soil samples in thawed and frozen states, allowed us to draw the following conclusions:

1. The radiation balance for Norilsk conditions from May to August is positive and leads to soil heating, and for the rest of the year, it is negative and leads to its cooling. The radiation balance and evaporation of moisture from the soil surface, when calculating its temperature, can be taken into account through a correction to the average monthly air temperature. In the summer months, this correction increases the average monthly air temperature to 3 °C, and in the winter months, on the contrary, it decreases the air temperature by 1–2 °C.
2. In the natural climatic conditions of Norilsk, the greatest thawing of the soil is observed in September, and the maximum depth of soil thawing is –1.25 m.
3. A decrease in the moisture content of the surface layers of soil is shown by a decrease in the influence of phase transitions on the thermal-inertial properties of the soil, which leads to an increase in the thickness of the active soil layer, where annual temperature fluctuations occur, to an increase in the depth of soil thawing in the summer-autumn period, and to a decrease in soil temperature below the active layer.
4. The absence of snow cover and direct solar radiation are factors that lead to a significant decrease in the temperature of soil under the ventilated basement of a multi-story residential building compared to natural conditions and a decrease in the maximum thawing depth in September to

–1.1 m. When selecting a ventilated basement design, it is important to ensure that the soil surface within the ventilated basement is protected from solar radiation in the summer and is not covered by snow in the winter.

5. For multi-story buildings with ventilated basements, individual structural elements, when insulating them, can be placed directly on the ground surface, without additional thawing of the soil underneath them. However, in this case, the absence of additional soil thawing must be confirmed by a thermal engineering calculation taking into account the thermal conditions in the rooms above the structural elements, the area ratio of the ventilated basement to the structure foundation, and their additional insulation from the ground surface. It should be noted that the optimal location for such structures is the central zone of the ventilated basement.

References

1. Obu, J. How Much of the Earth's Surface is Underlain by Permafrost? Journal of Geophysical Research: Earth Surface. 2021. 126(5). Article no. e2021JF006123. DOI: 10.1029/2021JF006123
2. Nevechnaya merzlota [Not permafrost]. [Online]. URL: https://porarctic.ru/ru/projects/geokrio (date of application: 17.06.25).
3. Anisimov, O., Badina, S., Beloluckaya, M., et al. Izmenenie klimata v Rossijskoj Arktike: riski i novye vozmozhnosti [Climate Change in the Russian Arctic: Risks and New Opportunities]. Skolkovo: Moscow School of Management, 2022. 105 p.
4. Biskaborn, B.K., Smith, S.L., Noetzli, J., Matthes, H., Vieira, G., Streletskiy, D., et al. Permafrost is warming at a global scale. Nature communications. 2019. 10(1). Article no. 264. DOI: 10.1038/s41467-018-08240-4
5. Malkova, G., Drozdov, D., Vasiliev, A., Gravis, A., Kraev, G., Korostelev, Y., et al. Spatial and Temporal Variability of Permafrost in the Western Part of the Russian Arctic. Energies. 2022. 15(7). Article no. 2311. DOI: 10.3390/en15072311
6. Masson-Delmotte, V., Zhai, P., et al. IPCC Special Report: Global Warming of 1.5 °C. Summary for Policymakers. World Meteorological Organization. Geneva, 2018. 32 p.
7. Osipov, V., Aksyutin, O., Sergeev, D., Tipenko, G., Ishkov, A. Using the Data of Geocryological Monitoring and Geocryological Forecast for Risk Assessment and Adaptation to Climate Change. Energies. 2022. 15(3). Article no. 879. DOI: 10.3390/en15030879
8. Jorgenson, M.T., Racine, C.H., Walters, J.C., Osterkamp, T.E. Permafrost Degradation and Ecological Changes Associated with a Warming Climate in Central Alaska. Climatic Change. 2001. 48(4). Pp. 551–579. DOI: 10.1023/A:1005667424292
9. McKenzie, J.M., Kurylyk, B.L., Walvoord, M.A., Bense, V.F., Fortier, D., Spence, C., Grenier, C. Invited perspective: What lies beneath a changing Arctic? The Cryosphere. 2021. 15(1). Pp. 479–484. DOI: 10.5194/tc-15-479-2021
10. Streletskiy, D.A., Suter, L.J., Shiklomanov, N.I., Porfiriev, B.N., Eliseev, D. O. Assessment of climate change impacts on buildings, structures and infrastructure in the Russian regions on permafrost. Environmental Research Letters. 2019. 14(2). Article no. 025003. DOI: 10.1088/1748-9326/aaf5e6
11. Hjort, J., Karjalainen, O., Aalto, J., Westermann, S., Romanovsky, V. E., Nelson, F.E., Etzelmüller, D., Luoto, M. Degrading permafrost puts Arctic infrastructure at risk by mid-century. Nature communications, 2018. 9(1). Article no. 5147. DOI: 10.1038/s41467-018-07557-4
12. Chuvilin, E., Sokolova, N., Bukhanov, B. Changes in Unfrozen Water Contents in Warming Permafrost Soils. Geosciences. 2022. 12(6). Article no. 253. DOI: 10.3390/geosciences12060253
13. Romanovsky, V.E., Drozdov, D.S., Oberman, N.G., Malkova, G.V., Kholodov, A.L., Marchenko, S.S., et al. Thermal state of permafrost in Russia. Permafrost and Periglacial Processes. 2010. 21(2). Pp. 136–155. DOI: 10.1002/ppp.683
14. Wang, L., Liu, J., Yu, X., Wang, T., Feng, R. A Simplified Model for the Phase Composition Curve of Saline Soils Considering the Second Phase Transition. Water Resources Research. 2021. 57(1). Article no. e2020WR028556. DOI: 10.1029/2020WR028556
15. Wang, D., Tighe, S.L., Yin, S. Preliminary Analysis of Permafrost Degradation in Ingraham Trail, Northwest Territories. Lecture Notes in Civil Engineering. 240: Proceedings of the Canadian Society of Civil Engineering Annual Conference 2021. CSCE 2021. Springer. Singapore, 2021. Pp. 109–121. DOI: 10.1007/978-981-19-0507-0_11
16. Vasiltsov, V.S., Vasiltsova, V.M. Strategic Planning of Arctic Shelf Development Using Fractal Theory Tools. Journal of Mining Institute. 2018. 234. Pp. 663–672. DOI: 10.31897/PMI.2018.6.663
17. Ershov, E.D. Geokriologiya SSSR. Evropejskaya territoriya SSSR [Geocryology of the USSR. European Territory of the USSR]. Moscow: Nedra, 1988. 358 p.
18. Ershov, E.D. Geokriologiya SSSR. Zapadnaya Sibir' [Geocryology of the USSR. Western Siberia]. Moscow: Nedra, 1989. 454 p.
19. Khrustalev, L.N., Parmuzin, S.Y., Emelyanova, L.V. Nadezhnost' severnoj infrastruktury v usloviyah menyayushchegosya klimata [Stability of northern infrastructure under changing climate]. Moscow: University Book Press, 2011. 342 p.
20. Mangushev, R.A., Karlov, V.D., Sakharov, I.I., Osokin, A.I. Osnovaniya i fundamenty [Foundations and Foundations: Textbook for Bachelors of Construction and Specialists in the Field of Construction of Unique Buildings and Structures]. ASV Publishing House, 2019. 468 p.
21. Buslaev, G., Tsvetkov, P., Lavrik, A., Kunshin, A., Loseva, E., Sidorov, D. Ensuring the Sustainability of Arctic Industrial Facilities under Conditions of Global Climate Change. 2021. 10(12). Article no. 128. DOI: 10.3390/ resources10120128
22. Peng, H., Ma, W., Mu, Y. H., Jin, L. Impact of permafrost degradation on embankment deformation of Qinghai-Tibet Highway in permafrost regions. Journal of Central South University. 2015. 22(3). Pp. 1079–1086. DOI: 10.1007/s11771-015-2619-2
23. Vasilev, G.G., Dzhalyabov, A.A., Leonovich, I.A. Analysis of the Causes of Engineering Structures Deformations at Gas Industry Facilities in the Permafrost Zone. Journal of Mining Institute. 2021. 249. Pp. 377–385. DOI: 10.31897/PMI.2021.3
24. Kotov, P., Stanilovskaya, J. Long-term strength of frozen saline soils. Magazine of Civil Engineering. 2022. 5(13). Article no. 11307. DOI: 10.34910/MCE.113.7
25. Stetjukha, V.A. Frost cracks formation in permafrost regions. Magazine of Civil Engineering. 2021. 4(104). Article no. 10405. DOI: 10.34910/MCE.104.5
26. Alekseev, A.G. Calculation of seasonal soil freezing depth by engineering and numerical methods. Bulletin of Science and Research Center of Construction. 2024. 42(3). Pp. 56–82. DOI: 10.37538/2224-9494-2024-3(42)-56-82

27. Borej 3D. Rukovodstvo pol'zovatelya [Boreas 3D. User's Guide]. Version 2024.3. 129 p.
28. Russian State Standard SP-25.13330.2020. Osnovaniyania I fundamenty na vechnomerzlykh gruntah [Soil bases and foundations on permafrost soils]. Moscow: Ministry of Construction of Russia, 2020. 110 p.
29. Budyko, M.I. Teplovoj balans zemnoj poverhnosti [The thermal balance of the Earth's surface]. Leningrad: Hydrometeorological Publishing House, 1956. 255 p.
30. Nauchno-prikladnoj spravochnik po klimatu SSSR. Mnogoletnie dannye [Scientific and applied handbook on the climate of the USSR. Long-term data]. Series 3. Parts. 1–6. Iss. 21: Krasnoyarskij kraj. Tuvinskaya ASSR [Krasnoyarsk Krai. Tuvan ASSR]. Book 1. Leningrad: Gidrometeoizdat, 1990. 623 p.
31. Pogoda v Noril'ske [Weather in Norilsk]. [Online]. URL: https://norilsk.ginfo.ru/pogoda (reference date: 17.06.2025).
32. Fedotov, A.A., Kaniber, V.V., Hrapov, P.V. Analysis and Forecasting of Changes in the Soil Temperature Distribution in the Area of the City of Norilsk. International Journal of Open Information Technologies. 2020. 8(10). Pp. 51–65.

Information about the authors:

***Mikhail Nizovtsev**, Doctor of Technical Sciences*
ORCID: https://orcid.org/0000-0003-2372-6544
E-mail: nizovtsev@itp.nsc.ru

***Aleksey Sterlyagov**, PhD in Technical Sciences*
ORCID: https://orcid.org/0000-0001-8443-6474
E-mail: 30j@mail.ru

Received 03.07.2025. Approved after reviewing 30.11.2025. Accepted 02.12.2025.